ACADEMIC PRESS

Available online at www.sciencedirect.com

SCIENCE DIRECT®

Journal of Sound and Vibration 263 (2003) 299–317

JOURNAL OF SOUND AND VIBRATION

www.elsevier.com/locate/jsvi

Vibration of a two-member open frame

G.R. Heppler[a,*], D.C.D. Oguamanam[b], J.S. Hansen[b]

[a] *Systems Design Engineering, University of Waterloo, 200 University Ave. West, Waterloo, Ont., Canada N2L 3G1*
[b] *Institute for Aerospace Studies, University of Toronto, 4925 Dufferin Street, Toronto, Ont., Canada M3H 5T6*

Received 26 November 2001; accepted 13 June 2002

Abstract

The dynamics of a two-member open frame structure undergoing both in- and out-of-plane motion is examined. The frames are modelled using the Euler–Bernoulli beam theory and are further generalized by permitting an arbitrary angle between the beams and the attachment of a payload at the end of the second beam. The equations of motion are derived using Hamilton's principle and the orthogonality conditions are presented. It is shown that the in- and out-of-plane motions can be decoupled by including the axial deformation components in the assumed displacement fields. The natural frequencies of the system and the contribution of each member into the system potential energy are examined via numerical examples.

1. Introduction

Frame structures can be categorized as closed or open [1]. Closed frames are frames formed by chains of beams in which both ends are fixed (e.g., Refs. [2–10]). The simplest example of a closed frame is a three-beam member portal frame, (e.g., Refs. [5–10]). Open frames are chains of beams that have one end fixed and the other end free (e.g., Refs. [1,11–14]). This paper is concerned with open frame structures. While the most common focus of frame analysis is civil engineering structures, the kind of structure being considered here has broader instances of application such as space-based antenna structures and electrical or electronic components operating in severe dynamic environments such as that might be found in a rocket launch.

The dynamics of two-member open frame structure which comprises a cantilever beam with a second beam attached to its free end has been considered by Bang [13], Oguamanam et al. [1] and Gürgöze [14]. Bang [13] and Gürgöze [14] examine L-shaped configurations without a tip mass

*Corresponding author. Fax: +1-519-746-4791.
E-mail address: heppler@solstice.uwaterloo.ca (G.R. Heppler).

0022-460X/03/$ - see front matter
PII: S0022-460X(02)01125-2

while Oguamanam et al. [1] investigate configurations with arbitrary inclination angles with or without a tip mass. Oguamanam et al. [1] define an angle of inclination measured from the undeformed axis of the fixed beam (the *first* beam) to the undeformed axis of the beam with the free end (the *second* or *distal* beam). They provide analytical expressions for the frequency (or characteristic) equation, the mode shapes, and the orthogonality conditions for the case of planar motion of the frame. In addition to the study being limited to in-plane motion, axial deformation was ignored.

The advantages and disadvantages of analytical solutions for L-shaped structures versus finite-dimensional approximations solutions have been presented by Bang [13]. Oguamanam et al. [1] further highlight the advantages of the analytical solution over the finite element method (FEM) using specific examples. In particular, a 60-degrees-of-freedom FEM model is used to obtain accurate results for the first five natural frequencies. The disadvantage of using this model in a control system is stressed.

This study extends the work by Oguamanam et al. [1] by relaxing the restrictions on the motion of the structure. The formulation technique used in that work is cumbersome in light of the relaxation introduced here. Hence a substructure approach is adopted. The in- and out-of-plane motions uncouple and the system reduces to solving two sets of governing equations of motion. Neither the analytical expression for the frequency equation nor the analytical expressions for the mode shapes are included in the paper because of their extreme length and complexity. Nevertheless, the components of the matrices that lead to the frequency equations and expressions for the mode shapes, for both the in- and out-of-plane motions, are presented. The orthogonality conditions are also included.

Numerical simulations are performed to examine the effects of: the ratio of the lengths of the beams, the ratio of the mass at the tip to the mass of the first beam, and the orientation angle on the natural frequencies. The contribution of each member to the system potential energy is also investigated.

2. Equations of motion

A global reference frame is attached at the base of the structure and a non-inertial frame is attached at the joint as depicted in Fig. 1. The unit vectors along the x_1-, y_1-, and z_1-axis of the fixed inertial frame $\mathscr{F}_a$ are, respectively, defined as $\mathbf{a}_1$, $\mathbf{a}_2$ and $\mathbf{a}_3$. Similarly, the unit vectors of the body fixed frame $\mathscr{F}_b$ are $\mathbf{b}_1$, $\mathbf{b}_2$ and $\mathbf{b}_3$ and they correspond to the x_2-, y_2-, and z_2-axis of the non-inertial frame $\mathscr{F}_b$ which has its origin at the junction of the two beam segments.

The assumed displacement field for the ith beam is given by

$$\bar{u}_i = u_i - z_i \frac{\partial w_i}{\partial x_i} - y_i \frac{\partial v_i}{\partial x_i}, \quad \bar{v} = v_i - z_i \psi_i, \quad \text{and} \quad \bar{w}_i = w_i + y_i \psi_i. \tag{1}$$

The system kinetic energy T is composed of three components, the contributions from the beams and the contribution of the tip mass (modelled as a point mass), so that

$$T = T_1 + T_2 + T_t, \tag{2}$$

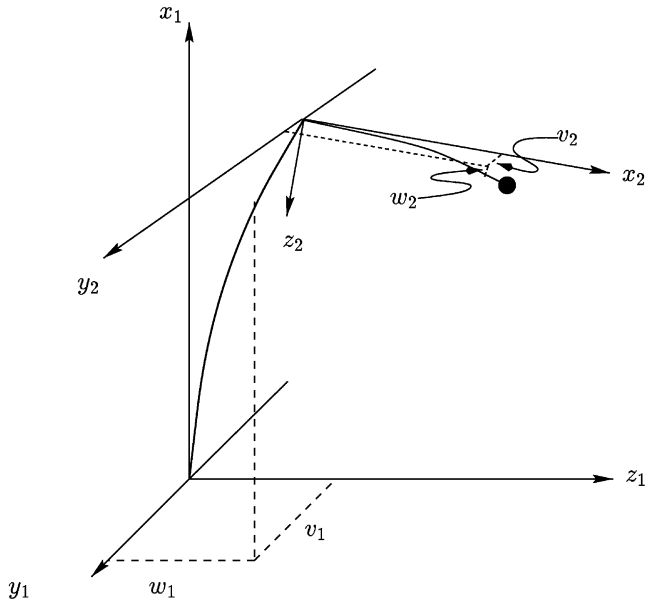

Fig. 1. Deformed schematic of the system.

where

$$T_i = \tfrac{1}{2}\rho_i A_i \int_0^{L_i} (\dot{u}_i^2 + \dot{v}_i^2 + \dot{w}_i^2)\,\mathrm{d}x_i + \tfrac{1}{2}\rho_i J_i \int_0^{L_i} \dot{\psi}_i^2\,\mathrm{d}x_i \quad \text{for } i = 1,2 \tag{3}$$

(rotatory inertia has been ignored) and

$$T_t = \tfrac{1}{2} m_t (\dot{u}_2^2(L_2,t) + \dot{v}_2^2(L_2,t) + \dot{w}_2^2(L_2,t)). \tag{4}$$

The system potential energy U is composed of a contribution from each beam segment and is given by

$$U = U_1 + U_2, \tag{5}$$

where

$$\begin{aligned} U_i = &\frac{1}{2}\int_0^{L_i} E_i A_i \left(\frac{\partial u_i}{\partial x_i}\right)^2 \mathrm{d}x_i + \frac{1}{2}\int_0^{L_i} E_i I_{yy}^{(i)} \left(\frac{\partial^2 w_i}{\partial x_i^2}\right)^2 \mathrm{d}x_i \\ &+ \frac{1}{2}\int_0^{L_i} E_i I_{zz}^{(i)} \left(\frac{\partial^2 v_i}{\partial x_i^2}\right)^2 \mathrm{d}x_i + \frac{1}{2}\int_0^{L_i} G_i J_i \left(\frac{\partial \psi_i}{\partial x_i}\right)^2 \mathrm{d}x_2 \quad \text{for } i = 1,2. \end{aligned} \tag{6}$$

Using T and U in Hamilton's principle and taking variations over the free variables u_i, v_i, w_i, and ψ_i will yield the governing equations of motion. The derivation will assume a cantilever frame where the end corresponding to $x_1 = 0$ is clamped such that the forced boundary conditions

will be

$$u_1(0,t)=0, \quad \psi_1(0,t)=0, \tag{7}$$

$$v_1(0,t)=0, \quad w_1(0,t)=0, \tag{8}$$

$$v_1'(0,t)=0, \quad w_1'(0,t)=0. \tag{9}$$

During the variation process it is necessary to make use of the geometric compatibility conditions at $x_1=L_1$ and $x_2=0$, i.e.

$$u_1(L_1,t)=u_2(0,t)\cos(\theta)-w_2(0,t)\sin(\theta), \quad \psi_1(L_1,t)=\psi_2(0,t)\cos(\theta)-v_2'(0,t)\sin(\theta), \tag{10}$$

$$v_1(L_1,t)=v_2(0,t), \quad v_1'(L_1,t)=\psi_2(0,t)\sin(\theta)+v_2'(0,t)\cos(\theta), \tag{11}$$

$$w_1(L_1,t)=u_2(0,t)\sin(\theta)+w_2(0,t)\cos(\theta), \quad w_1'(L_1,t)=w_2'(0,t). \tag{12}$$

Subsequently, the governing equations of motion are found to be, for $i=1,2$,

$$\rho_i A_i \ddot{u}_i - E_i A_i \frac{\partial^2 u_i}{\partial x_i^2}=0, \quad \rho_i A_i \ddot{v}_i + E_i I_{zz}^{(i)} \frac{\partial^4 v_i}{\partial x_i^4}=0,$$

$$\rho_i A_i \ddot{w}_i + E_i I_{yy}^{(i)} \frac{\partial^4 w_i}{\partial x_i^4}=0, \quad \rho_i A_i \ddot{\psi}_i - G_i J_i \frac{\partial^2 \psi_i}{\partial x_i^2}=0, \tag{13}$$

with the following additional force and moment compatibility conditions at ($x_1=L_1,\ x_2=0$):

$$E_1 I_{yy}^{(1)} w_1'''(L_1,t)\sin(\theta)-E_1 A_1 u_1'(L_1,t)\cos(\theta)+E_2 A_2 u_2'(0,t)=0, \tag{14}$$

$$E_1 I_{zz}^{(1)} v_1'''(L_1,t)-E_2 I_{zz}^{(2)} v_2'''(0,t)=0, \tag{15}$$

$$E_1 I_{yy}^{(1)} w_1'''(L_1,t)\cos(\theta)+E_1 A_1 u_1'(L_1,t)\sin(\theta)-E_2 I_{yy}^{(2)} w_2'''(0,t)=0, \tag{16}$$

$$E_1 I_{zz}^{(1)} v_1''(L_1,t)\sin(\theta)+G_1 J_1 \psi_1'(L_1,t)\cos(\theta)-G_2 J_2 \psi_2'(0,t)=0, \tag{17}$$

$$E_1 I_{zz}^{(1)} v_1''(L_1,t)\cos(\theta)-G_1 J_1 \psi_1'(L_1,t)\sin(\theta)-E_2 I_{zz}^{(2)} v_2''(0,t)=0, \tag{18}$$

$$E_1 I_{yy}^{(1)} w_1''(L_1,t)-E_2 I_{yy}^{(2)} w_2''(0,t)=0. \tag{19}$$

The natural boundary conditions at the free end ($x_2=L_2$) are

$$v_2''(L_2,t)=0, \quad E_2 I_{zz}^{(2)} v_2'''(L_2,t)-m_t \ddot{v}_2(L_2,t)=0, \tag{20}$$

$$w_2''(L_2,t)=0, \quad E_2 I_{yy}^{(2)} w_2'''(L_2,t)-m_t \ddot{w}_2(L_2,t)=0, \tag{21}$$

$$\psi_2'(L_2,t)=0, \quad E_2 A_2 u_2'(L_2,t)+m_t \ddot{u}_2(L_2,t)=0. \tag{22}$$

3. Frequency equation

To reduce the number of defining parameters the following non-dimensional variables are introduced:

$$\xi_i = \frac{x_i}{L_i}, \quad \rho = \frac{\rho_2 A_2}{\rho_1 A_1}, \quad M_t = \frac{m_t}{\rho_1 A_1 L_1}, \quad L = \frac{L_2}{L_1},$$
$$\lambda_{ui}^2 = \frac{\rho_i L_i^2 \omega^2}{E_i}, \quad \lambda_{vi}^4 = \frac{\rho_i A_i L_i^4 \omega^2}{E_i I_{zz}^{(i)}}, \quad \lambda_{wi}^4 = \frac{\rho_i A_i L_i^4 \omega^2}{E_i I_{yy}^{(i)}}, \quad \lambda_{\psi i}^2 = \frac{\rho_i L_i^2 \omega^2}{G_i},$$
$$\sigma = \frac{E_2 A_2}{E_1 A_1}, \quad \eta = \frac{G_2 J_2}{G_1 J_1}, \quad v_{vi} = \frac{I_{zz}^{(i)}}{A_i L_i^2}, \quad v_{wi} = \frac{I_{yy}^{(i)}}{A_i L_i^2}, \quad \chi_i = \frac{E_i I_{zz}^{(i)}}{G_i J_i}. \tag{23}$$

By assuming a separable solution in the form ($i = 1, 2$)

$$u_i(x_i, t) = L_i U_i(\xi_i) e^{j\omega t}, \quad v_i(x_i, t) = L_i V_i(\xi_i) e^{j\omega t},$$
$$w_i(x_i, t) = L_i W_i(\xi_i) e^{j\omega t}, \quad \psi_i(x_i, t) = \Psi_i(\xi_i) e^{j\omega t}, \tag{24}$$

the equations of motion can be written as ($i = 1, 2$)

$$U_i'' + \lambda_{ui}^2 U_i = 0, \tag{25}$$

$$V_i'''' - \lambda_{vi}^4 V_i = 0, \tag{26}$$

$$W_i'''' - \lambda_{wi}^4 W_i = 0, \tag{27}$$

$$\Psi_i'' + \lambda_{\psi i}^2 \Psi_i = 0. \tag{28}$$

In light of the non-dimensionalization and the separation of variables, the boundary conditions can be expressed as

$$U_1(0) = 0, \quad V_1(0) = 0, \quad W_1(0) = 0, \tag{29}$$

$$\Psi(0) = 0, \quad V_1'(0) = 0, \quad W_1'(0) = 0, \tag{30}$$

$$V_2''(1) = 0, \quad W_2''(1) = 0, \quad \Psi_2'(1) = 0, \tag{31}$$

$$\rho L U_2'(1) - M_t \lambda_{u2}^2 U_2(1) = 0, \quad \rho L V_2'''(1) + M_t \lambda_{v2}^4 V_2(1) = 0,$$
$$\rho L W_2'''(1) + M_t \lambda_{w2}^4 W_2(1) = 0 \tag{32}$$

and the geometric compatibility equations can be expressed as

$$U_1(1) - L U_2(0) \cos(\theta) + L W_2(0) \sin(\theta) = 0, \tag{33}$$

$$V_1(1) - L V_2(0) = 0, \tag{34}$$

$$W_1(1) - L U_2(0) \sin(\theta) - L W_2(0) \cos(\theta) = 0, \tag{35}$$

$$\Psi_1(1) - \Psi_2(0) \cos(\theta) + V_2'(0) \sin(\theta) = 0, \tag{36}$$

$$V_1'(1) - \Psi_2(0)\sin(\theta) - V_2'(0)\cos(\theta) = 0, \tag{37}$$

$$W_1'(1) - W_2'(0) = 0, \tag{38}$$

$$v_{w1} W_1'''(1)\sin(\theta) - U_1'(1)\cos(\theta) + \sigma U_2'(0) = 0, \tag{39}$$

$$v_{v1} V_1'''(1) - \sigma v_{v2} V_2'''(0) = 0, \tag{40}$$

$$v_{w1} W_1'''(1)\cos(\theta) + U_1'(1)\sin(\theta) - \sigma v_{w2} W_2'''(0) = 0, \tag{41}$$

$$\chi_1 L V_1''(1)\sin(\theta) + L\Psi_1'(1)\cos(\theta) - \eta\Psi_2'(0) = 0, \tag{42}$$

$$\chi_1 L V_1''(1)\cos(\theta) - L\Psi_1'(1)\sin(\theta) - \chi_2\eta V_2''(0) = 0, \tag{43}$$

$$v_{w1} W_1''(1) - \sigma v_{w2} L W_2''(0) = 0. \tag{44}$$

The general solutions to the equations of motion (25)–(28) are

$$U_i(\xi_i) = B_1^{(i)}\cos(\lambda_{ui}\xi_i) + B_2^{(i)}\sin(\lambda_{ui}\xi_i), \tag{45}$$

$$V_i(\xi_i) = C_1^{(i)}\sin(\lambda_{vi}\xi_i) + C_2^{(i)}\cos(\lambda_{vi}\xi_i) + C_3^{(i)}\sinh(\lambda_{vi}\xi_i) + C_4^{(i)}\cosh(\lambda_{vi}\xi_i), \tag{46}$$

$$W_i(\xi_i) = D_1^{(i)}\sin(\lambda_{wi}\xi_i) + D_2^{(i)}\cos(\lambda_{wi}\xi_i) + D_3^{(i)}\sinh(\lambda_{wi}\xi_i) + D_4^{(i)}\cosh(\lambda_{wi}\xi_i) \tag{47}$$

and

$$\Psi_i(\xi_i) = F_1^{(i)}\cos(\lambda_{\psi i}\xi_i) + F_2^{(i)}\sin(\lambda_{\psi i}\xi_i), \tag{48}$$

respectively.

From Eqs. (29)–(30) the following may be deduced:

$$\begin{aligned} &B_1^{(1)} = 0, \quad C_2^{(1)} = -C_4^{(1)}, \quad C_1^{(1)} = -C_3^{(1)}, \\ &F_1^{(1)} = 0, \quad D_2^{(1)} = -D_4^{(1)}, \quad D_1^{(1)} = -D_3^{(1)}, \end{aligned} \tag{49}$$

hence

$$U_1(\xi_1) = B_2^{(1)}\sin(\lambda_{u1}\xi_1), \tag{50}$$

$$V_1(\xi_1) = C_1^{(1)}(\sin(\lambda_{v1}\xi_1) - \sinh(\lambda_{v1}\xi_1)) + C_2^{(1)}(\cos(\lambda_{v1}\xi_1) - \cosh(\lambda_{v1}\xi_1)). \tag{51}$$

$$W_1(\xi_1) = D_1^{(1)}(\sin(\lambda_{w1}\xi_1) - \sinh(\lambda_{w1}\xi_1)) + D_2^{(1)}(\cos(\lambda_{w1}\xi_1) - \cosh(\lambda_{w1}\xi_1)), \tag{52}$$

$$\Psi_1(\xi_1) = F_2^{(1)}\sin(\lambda_{\psi 1}\xi_1). \tag{53}$$

Eqs. (50) and (53) and the corresponding equations for the second beam (obtained from Eqs. (45)–(48) with $i = 2$) are substituted into the remaining boundary conditions (i.e., Eqs. (31)–(44)), and after some algebra yield 18 homogeneous equations which are linear in the unknown coefficients of integration. These equations can be expressed in matrix format as

$$[\mathbf{A}]_{18\times 18}\{\mathbf{q}\}_{18\times 1} = \{\mathbf{0}\}_{18\times 1}, \tag{54}$$

where

$$\{\mathbf{q}\} = [B_2^{(1)}, C_1^{(1)}, C_2^{(1)}, D_1^{(1)}, D_2^{(1)}, F_2^{(1)}, B_1^{(2)}, B_2^{(2)}, C_1^{(2)}, C_2^{(2)}, C_3^{(2)}, C_4^{(2)}, D_1^{(2)}, D_2^{(2)}, D_3^{(2)}, D_4^{(2)}, F_1^{(2)}, F_2^{(2)}]^{\mathrm{T}}.$$

The non-dimensional equations of motion (25)–(28) and the boundary conditions (29)–(32) show that the in- and out-of-plane motions are uncoupled. Therefore, the matrix $\mathbf{A}$ and vector $\mathbf{q}$ can be partitioned as

$$\begin{bmatrix} [\mathbf{A}_I] & \mathbf{0} \\ \mathbf{0} & [\mathbf{A}_O] \end{bmatrix} \begin{Bmatrix} \mathbf{q}_I \\ \mathbf{q}_O \end{Bmatrix}, \tag{55}$$

where the $\mathbf{A}_I$ and $\mathbf{q}_I$ refer to the in-plane components and $\mathbf{A}_O$ and $\mathbf{q}_O$ refer to the out-of-plane components, respectively. The vector component for the in-plane motion are

$$\{\mathbf{q}_I\} = [B_2^{(1)}, D_1^{(1)}, D_2^{(1)}, B_1^{(2)}, B_2^{(2)}, D_1^{(2)}, D_2^{(2)}, D_3^{(2)}, D_4^{(2)}]^{\mathrm{T}}$$

and for the out-of-plane motion are

$$\{\mathbf{q}_O\} = [C_1^{(1)}, C_2^{(1)}, F_2^{(1)}, C_1^{(2)}, C_2^{(2)}, C_3^{(2)}, C_4^{(2)}, F_1^{(2)}, F_2^{(2)}]^{\mathrm{T}}.$$

The entries for the matrices $\mathbf{A}_I$ and $\mathbf{A}_O$ are listed in Appendix A.

The uncoupling of the in-plane and the out-of-plane motions is realized because of the inclusion of the axial deformation components in the initial assumed displacement field, Eqs. (1). Given that the in- and out-of-plane motions are uncoupled, the natural frequencies of the system are determined by independently solving the characteristic equation that results from $\mathbf{A}_I$ and $\mathbf{A}_O$.

The explicit expression for the characteristic equation for the system in in-plane motion has previously been presented by Oguamanam et al. [1]. The corresponding expressions for the in-plane motion mode shapes were also presented. Axial effects were, however, ignored. The characteristic equation for the in-plane motion is not provided here because the inclusion of axial deformation complicates the expression to such an extent that nothing can be deduced with ease or certainty. However, the examples shown in the work presented by Alexandropoulos et al. [2], Kounadis and Meskouris [3], and Sophianopoulos and Kounadis [4] clearly show that, in closed frames, the contribution of the axial deflections to the mode shapes is substantial and there is no reason to believe that this will be different for the open frames considered here. The same argument holds for the out-of-plane motion.

4. Orthogonality conditions

The orthogonality conditions are derived using the equations of motion (13), the boundary conditions (7) and (20)–(22), and the compatibility conditions (10)–(12) and (14)–(19). The resulting expression for the in-plane motion can be expressed as

$$m_t L_2^2 (U_{2i}(1) U_{2j}(1) + W_{2i}(1) W_{2j}(1)) + \sum_{k=1}^{2} \rho_k A_k L_k^3 \int_0^1 (U_{ki} U_{kj} + W_{ki} W_{kj}) \, \mathrm{d}x_k = 0 \tag{56}$$

and that for the out-of-plane motion may be written as

$$m_t L_2^2 V_{2i}(1) V_{2j}(1) + \sum_{k=1}^{2} \rho_k L_k \int_0^1 (A_k L_k^2 V_{ki} V_{kj} + J_k \Psi_{ki} \Psi_{kj}) \, \mathrm{d}x_k = 0. \tag{57}$$

5. Numerical examples

The following examples have been chosen with several objectives in mind. The first is simply to confirm the formulation by making comparison to previous results. The second is to illustrate the effect that changing the relative lengths of the beams, while maintaining a constant system mass, has on the frequency behavior of the system. The third is to explore the effect that changing the size of the tip mass has on the frequency behavior of the system for a fixed value of L.

5.1. Example 1

The results presented in this example are meant to confirm both the formulation and the numerical results that arise from the formulation. Figs. 2 and 3 show the in- and out-of-plane

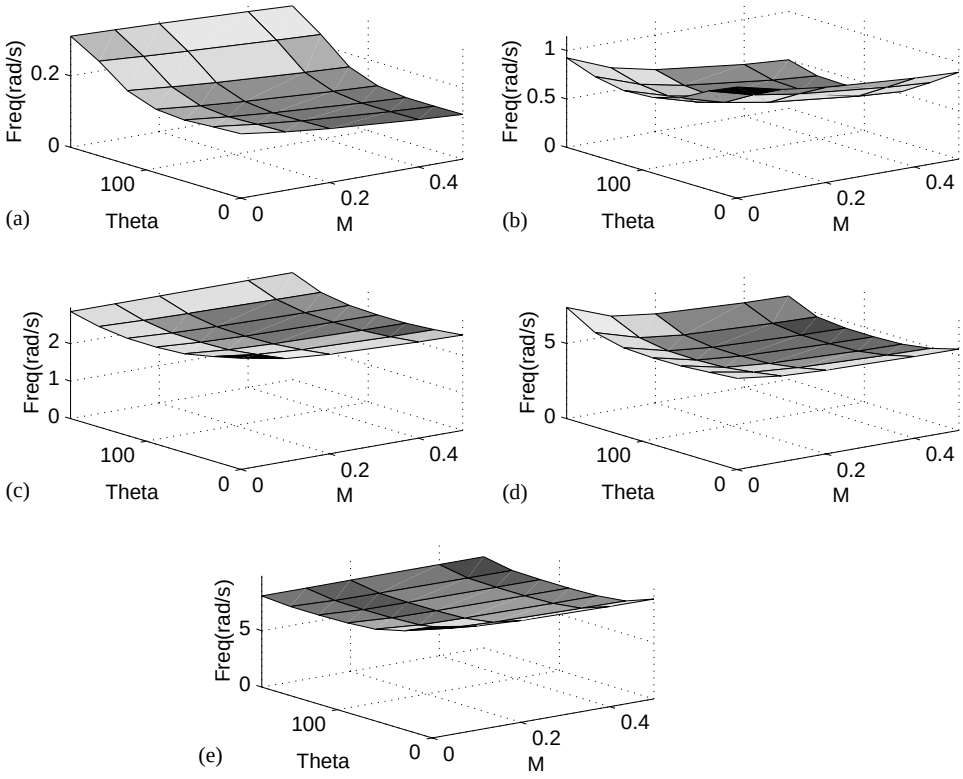

Fig. 2. In-plane modal frequencies versus M and θ: (a) Mode 1, (b) Mode 2, (c) Mode 3, (d) Mode 4, and (e) Mode 5.

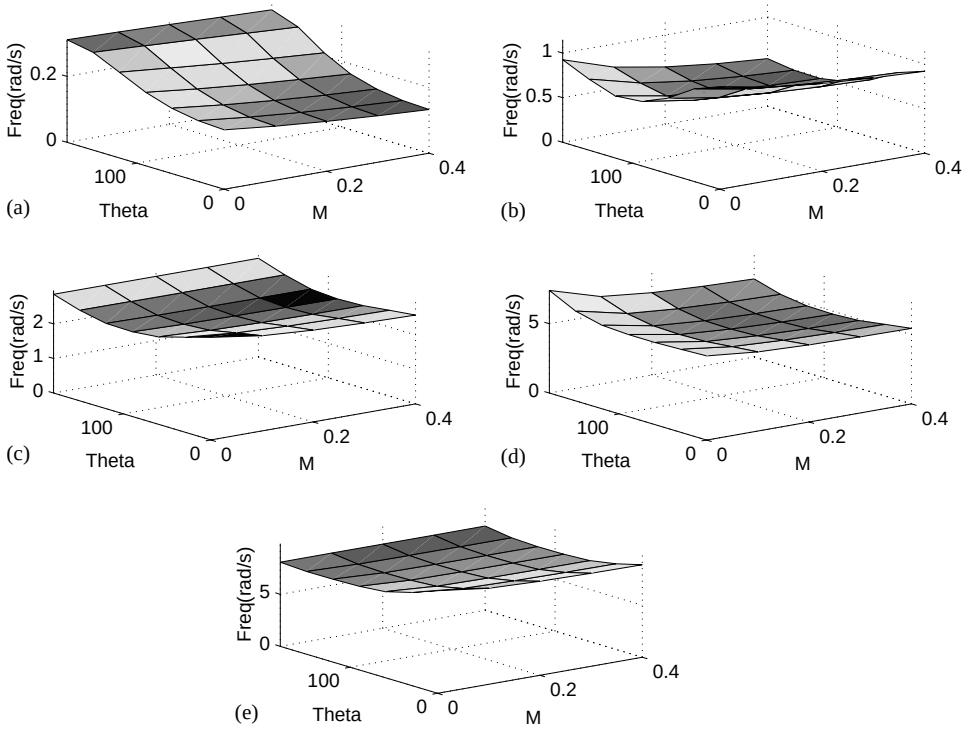

Fig. 3. Out-of-plane modal frequencies versus M and θ: (a) Mode 1, (b) Mode 2, (c) Mode 3, (d) Mode 4, and (e) Mode 5.

frequencies, respectively, obtained when the material and geometry parameters used first by Bang [13] and subsequently by Oguamanam et al. [1] are used in the present formulation. It should be noted that these particular values are representative of an orbiting antenna structure and are not intended to be representative of Earth-based engineering structures. As mentioned previously, the inclusion of the axial deflection allows the in- and out-of-plane modes to uncouple. Although they are uncoupled, it is observed that when $\theta = 0$ and π there are repeated frequencies where the in- and out-of-plane values are equal. The repeated values occur because the assumed geometry is a beam with equal moments of inertia about both principle cross-sectional axes and in these two configurations of θ repeated frequencies should be observed. For any given angle θ and tip-mass value M_t the in-plane frequency is always less than the corresponding (i.e., first, second, third, etc.) out-of-plane frequency. The data presented in Fig. 2 agree perfectly with those obtained from the strictly planar formulation [1]. Comparison of these two figures shows that, for the most part, there are no large differences in the magnitudes of the frequencies (in plane as compared to out of plane) nor in their behavior with changes in the magnitude of the tip mass.

5.2. *Example 2*

In this example, the material parameters have been chosen to correspond to those of aluminum, as given in Table 1 with the geometry of the two beams still implicitly given by the data used in Example 1.

Table 1
Material properties and non-dimensional parameters

ρ_1	2770 kg/m^3
ρ_2	2770 kg/m^3
ρ	1
$\rho_1 A_1$	4.5×10^{-3} kg/m^1
$\rho_2 A_2$	6.0×10^{-3} kg/m^1
E_1	70 GPa
E_2	70 GPa
$E_1 I_{yy_1}$	2.67×10^{-2} Nm^2
$E_1 I_{zz_1}$	2.67×10^{-2} Nm^2
$E_2 I_{yy_2}$	1.47×10^{-2} Nm^2
$E_2 I_{zz_2}$	1.47×10^{-2} Nm^2
G_1	30 GPa
G_2	30 GPa

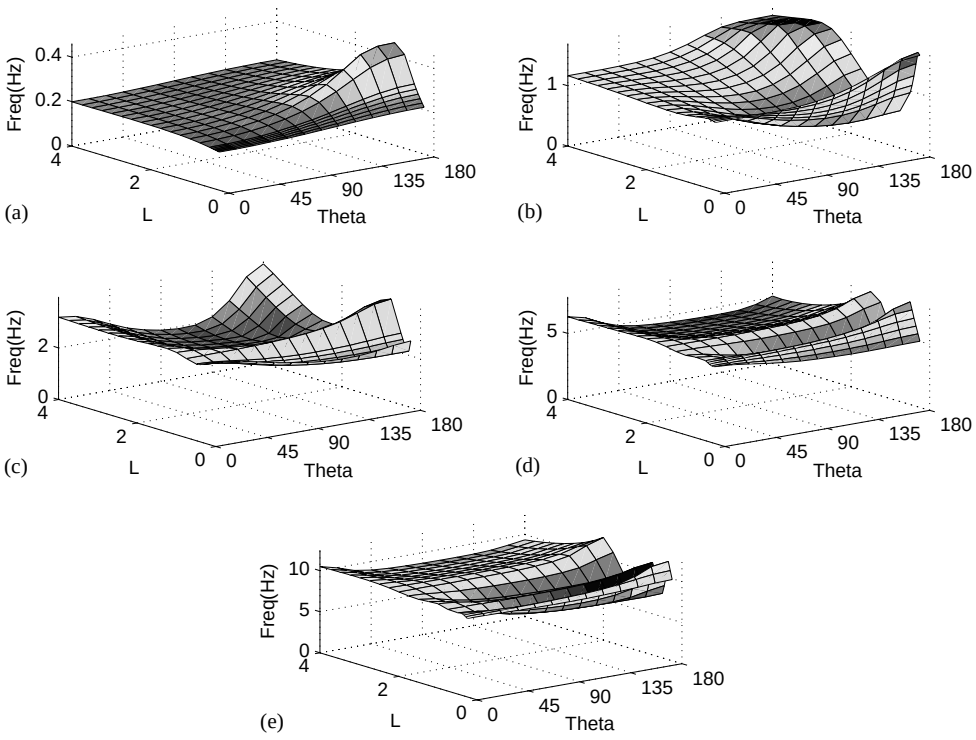

Fig. 4. In-plane modal frequencies versus L and θ: (a) Mode 1, (b) Mode 2, (c) Mode 3, (d) Mode 4, and (e) Mode 5.

The effect of varying the relative lengths of the two beams, while conserving total system mass and in the absence of a tip mass, is presented in Figs. 4 and 5. Fig. 4 shows the behavior of the frequencies associated with the in-plane modes and Fig. 5 provides the corresponding information

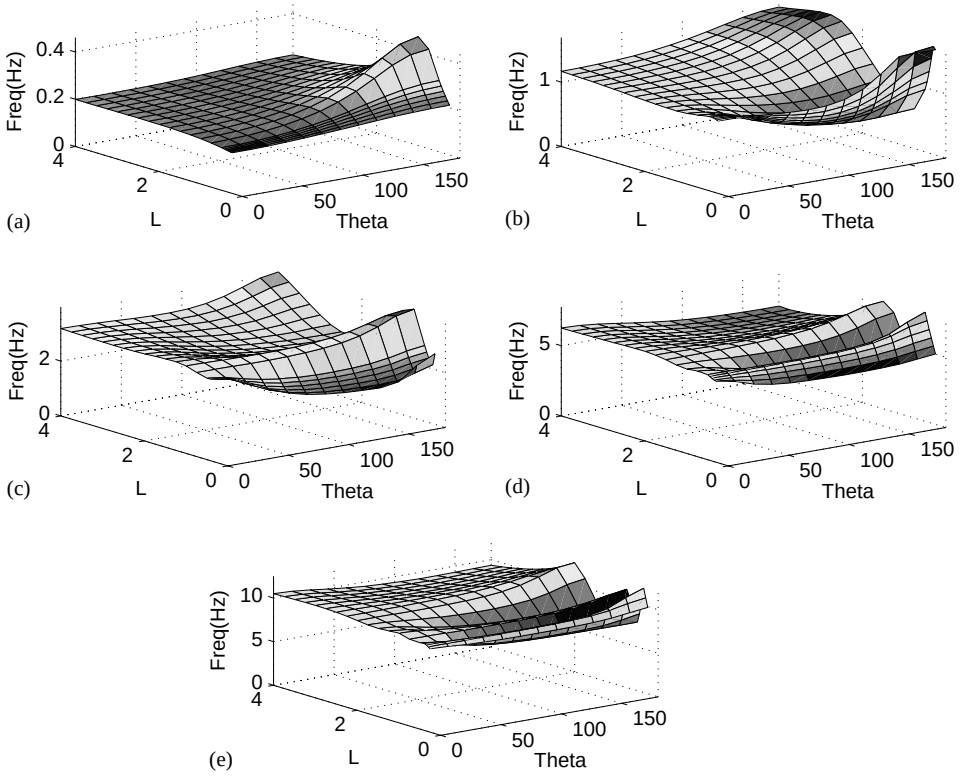

Fig. 5. Out-of-plane modal frequencies versus L and θ: (a) Mode 1, (b) Mode 2, (c) Mode 3, (d) Mode 4, and (e) Mode 5.

for the out-of-plane modes. As in the first example, both sets of figures are similar in terms of frequency magnitudes and general shape of the surfaces. As expected, when $\theta = 0$ and π the in- and out-of-plane frequencies are identical. The in-plane frequencies are slightly higher than the out-of-plane frequencies for a given θ–L pair. The difference is greatest for large values of L and actually reverses itself for small values of L when $\theta \approx \pi/4$. With respect to the first frequency in each configuration it may be observed that the configurations with the largest values of the first natural frequency have L close to unity and θ close to π. The lowest values of the first natural frequency correspond to small values of both L and θ. What is different, as compared to the first example, is the non-uniform dependence of the frequencies as a function of the length ratio L. The figures show that there are $n/2$ waves in the L direction for the nth frequency. These waves are more pronounced for large values of θ and they have a higher instantaneous frequency for small values of L. Examination of the frequency equation has not provided any definitive answers regarding the reason for this behavior.

Graphical representation of the mode shapes that correspond to a sample of the cases covered by Figs. 4 and 5 is not easy to present, nor would it be necessarily useful. For example, in [1] the illustrated mode shapes suggest that the distal beam has very little deformation in the first mode, and that consequently the majority of the modal strain energy is in the first beam. The validity of this conjecture cannot be determined from the illustrated mode shapes. To obtain some intuition about how the modal strain energy is distributed between the two beams consider Figs. 6–9. These

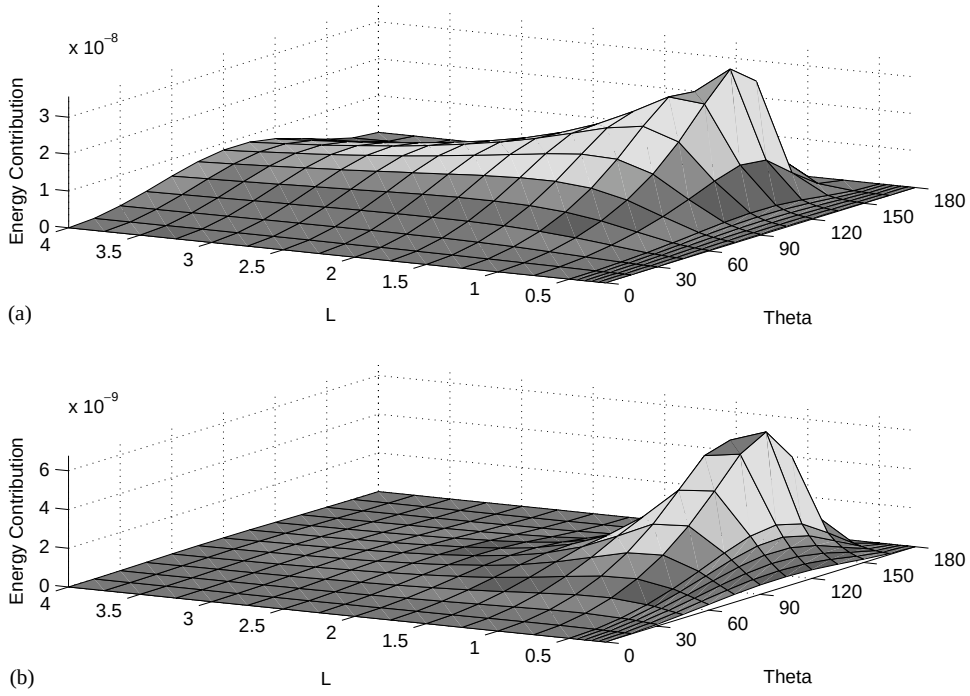

Fig. 6. In-plane axial strain energy, first mode, no tip mass: (a) Beam 1, and (b) Beam 2.

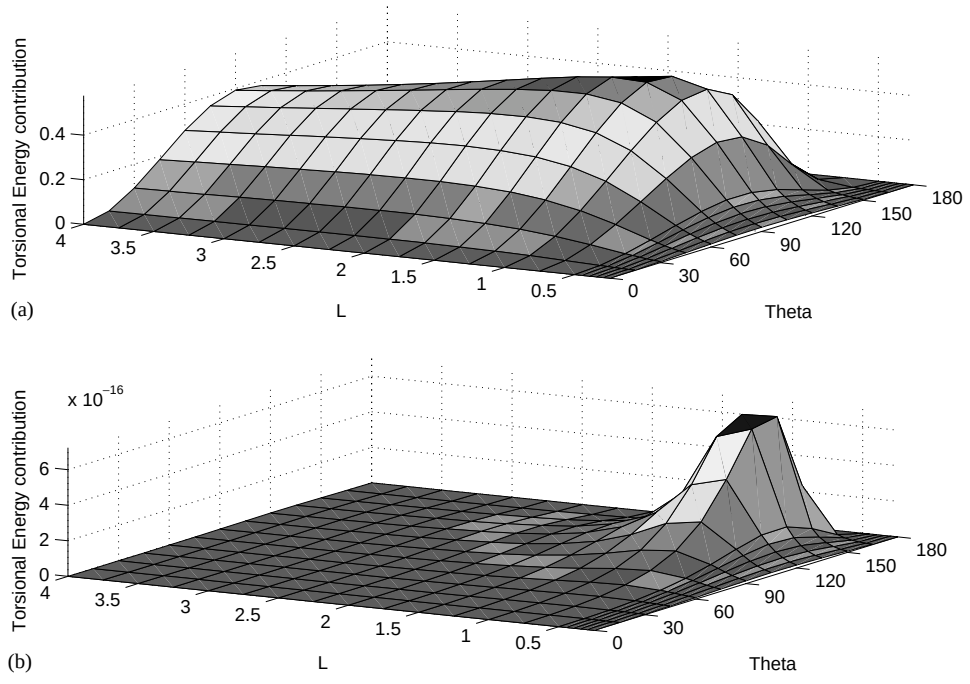

Fig. 7. Out-of-plane torsional strain energy, first mode, no tip mass: (a) Beam 1, and (b) Beam 2.

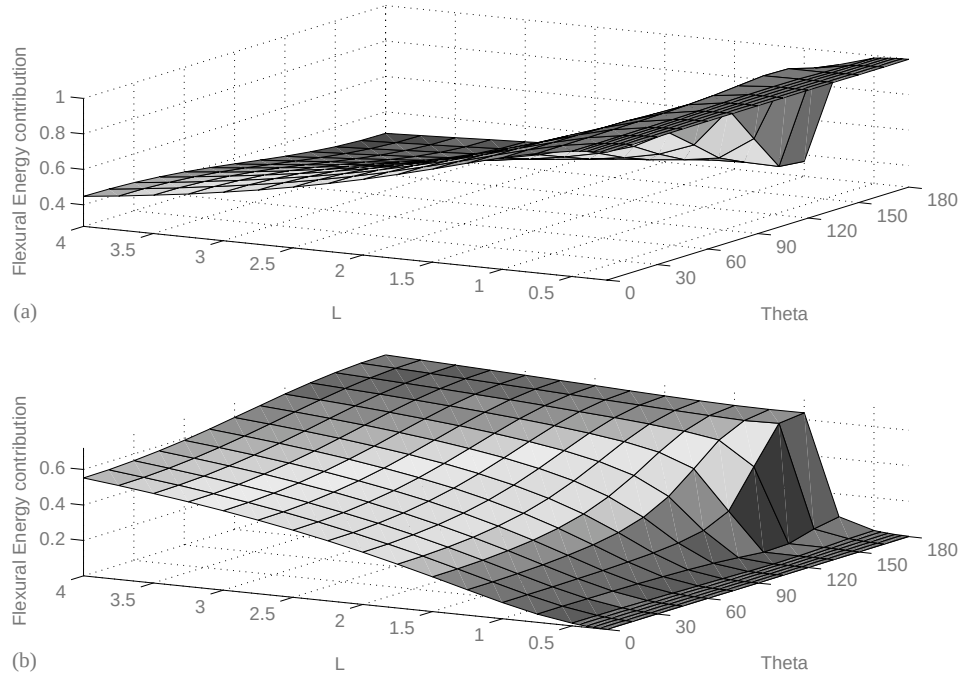

Fig. 8. In-plane flexural strain energy, first mode, no tip mass: (a) Beam 1, and (b) Beam 2.

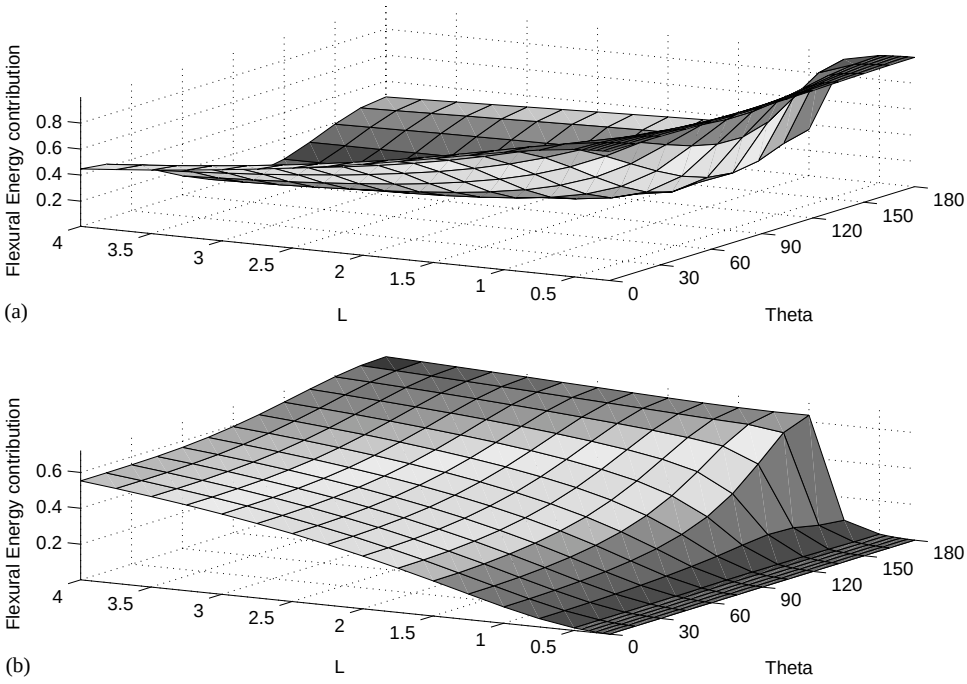

Fig. 9. Out-of-plane flexural strain energy, first mode, no tip mass: (a) Beam 1, and (b) Beam 2.

figures present the relative modal strain energy components as they are distributed between the first and second beam. The relative strain energy values presented in these figures are the ratio of the in-plane (out-of-plane) strain energy in beam one (two) divided by the total in-plane (out-of-plane) strain energy of the system.

Fig. 6 presents the distribution of the axial part of the modal strain energy for the in-plane part of the formulation. It is evident from the scale that very little of the total strain energy (less than $10^{-6}\%$) goes toward axial deformations. The out-of-plane part of the formulation provides non-flexural strain energy contributions for the two beams as shown in Fig. 7 where it may be observed that the second beam contributes virtually nothing to the total strain energy but the first beam does have a significant contribution. This is dominantly torsional strain energy and is greatest in the first beam due to the large eccentric inertia provided by the second beam. It is clearly illustrated in these figures that when the second beam is very short the torsional modal strain energy becomes negligible, as would be expected.

The out-of-plane flexural strain energy contribution is illustrated in Fig. 9 where it may be observed that the strain energy distribution between the two beams is complementary with respect to their relative lengths L. When the second beam is short ($L \approx 0$) virtually all of the bending strain energy is concentrated in the first beam and as the length of the second beam increases (i.e., L becoming larger) the proportion of the bending strain energy in the first beam diminishes and the portion in the second beam increases.

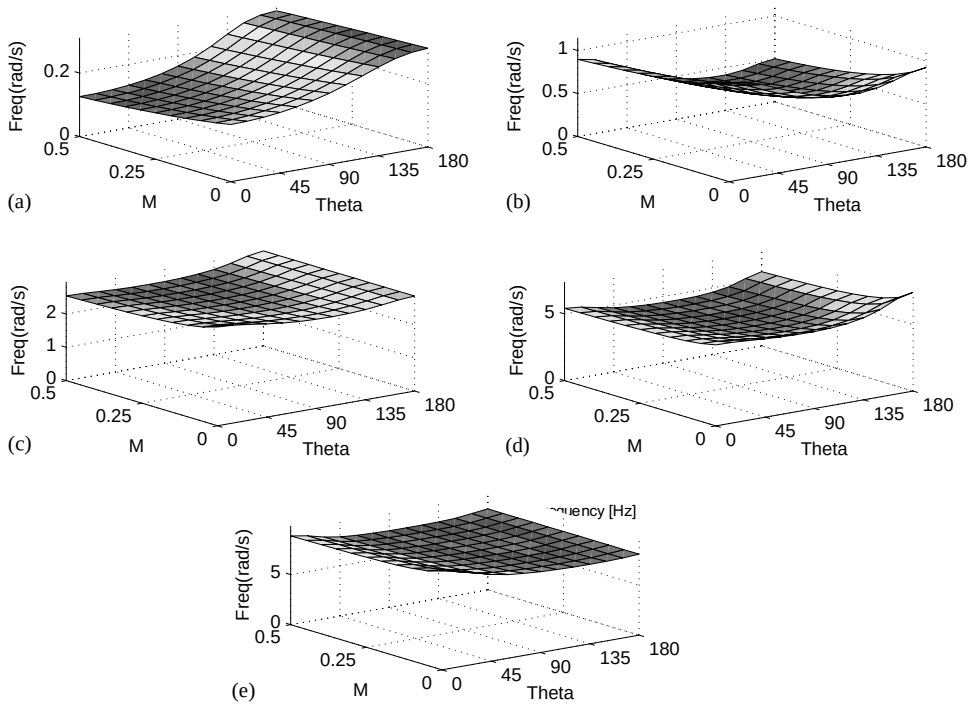

Fig. 10. In-plane modal frequencies versus M and θ: (a) Mode 1, (b) Mode 2, (c) Mode 3, (d) Mode 4, and (e) Mode 5.

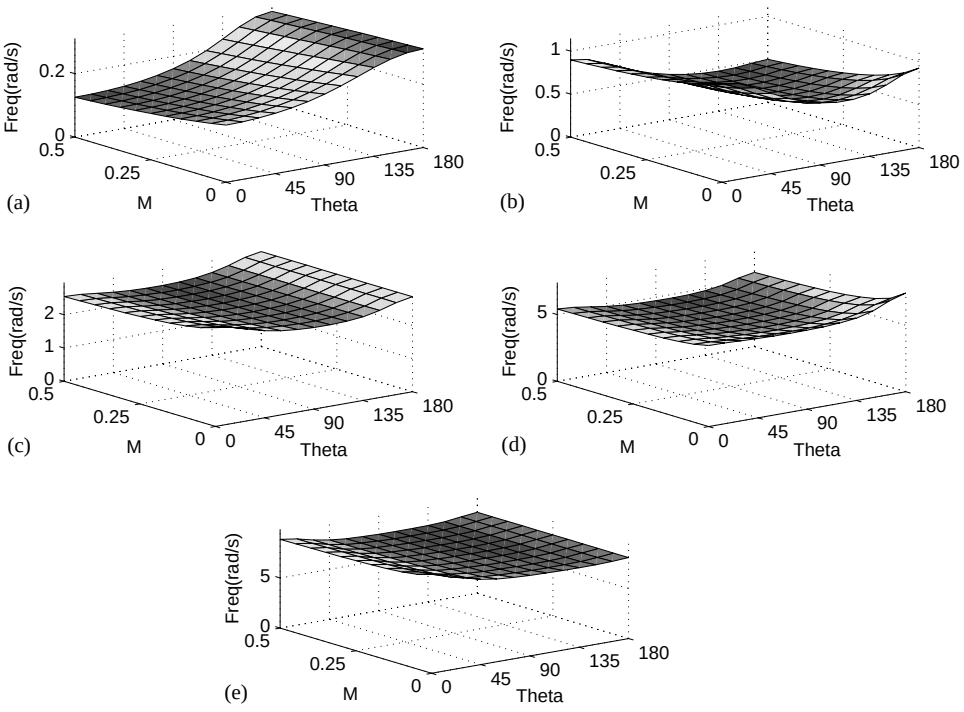

Fig. 11. Out-of-plane modal frequencies versus M and θ: (a) Mode 1, (b) Mode 2, (c) Mode 3, (d) Mode 4, and (e) Mode 5.

5.3. *Example 3*

In this example, the material parameters remain the same as those used in Example 2 (Table 1) with the geometry of the two beams still implicitly given by the data used in Example 1.

The effect of varying the magnitude of the tip-mass parameter such that $0 \leqslant M_t \leqslant 0.5$ is investigated for the single value of $L = 2.215/4.249 = 0.5213$ that was used by Bang [13]. Fig. 10 shows the behavior of the first five natural frequencies associated with the in-plane modes and Fig. 11 provides the corresponding information for the out-of-plane modes. As in the second example, both sets of figures are similar in terms of frequency magnitudes and general shape of the surfaces. The lowest frequencies correspond to small angles and large tip masses and the largest frequencies correspond to large angles and small masses. Regardless of the value of θ, the larger the tip mass the lower the frequencies, as expected.

6. Summary

It has been shown that inclusion of the axial deformation component in the assumed displacement field for the two beams ultimately allows the in- and out-of-plane frequency equations to be uncoupled and solved independently. The first five frequencies, in the examples

presented, support the expectation that they are dominated by either bending or torsion and there is no significant axial component in them. Therefore, while its inclusion in the formulation has provided analytical benefits the presence of the axial deformation components does not interfere with the calculation of the dominant frequencies of the structure.

The examples demonstrate that the first in-plane mode is a bending mode with the first beam dominating the mode for small values of L ($L<\frac{1}{2}$) with very little bending of the second beam in that range of values of L and for all θ. For larger values of L, the flexural parts of the first in-plane mode are complementary between beam one and beam two as L and θ change.

The out-of-plane modes are more dependent on L and θ with the first mode exhibiting a large torsional component in the first beam, except for very small values of L, and no significant torsional contribution in the second beam for any L, θ pair. The flexural parts of the first out-of-plane mode do not display the same form of complementary behavior exhibited by the first in-plane mode because of the torsional contribution present in the out-of-plane case. The bending contribution of the first beam, in the out-of-plane case, diminishes symmetrically about $\theta = \pi/2$ corresponding to a complementary increase in the torsional contribution in that range of angles. The bending contribution of the second beam is most prevalent for large values of both L and θ because in this region neither the first beam nor the second beam contribute much by way of either bending or torsion.

Appendix A. Entries of matrices $\mathbf{A}_I$ and $\mathbf{A}_O$

Using the notation that

$$S_\theta = \sin(\theta), \quad C_\theta = \cos(\theta), \quad s_{u1} = \sin(\lambda_{u1}), \quad c_{u1} = \cos(\lambda_{u1}),$$

$$s_{w1} = \sin(\lambda_{w1}), \quad c_{w1} = \cos(\lambda_{w1}), \quad sh_{w1} = \sinh(\lambda_{w1}), \quad ch_{w1} = \cosh(\lambda_{w1}),$$

$$s_{u2} = \sin(\lambda_{u2}), \quad c_{u2} = \cos(\lambda_{u2}), \quad s_{w2} = \sin(\lambda_{w2}), \quad c_{w2} = \cos(\lambda_{w2}),$$

$$sh_{w2} = \sinh(\lambda_{w2}), \quad ch_{w2} = \cosh(\lambda_{w2}), \quad s_{\psi_1} = \sin(\lambda_{\psi_1}), \quad c_{\psi_1} = \cos(\lambda_{\psi_1}),$$

$$s_{v1} = \sin(\lambda_{v1}), \quad c_{v1} = \cos(\lambda_{v1}), \quad sh_{v1} = \sinh(\lambda_{v1}), \quad ch_{v1} = \cosh(\lambda_{v1}),$$

$$s_{\psi_2} = \sin(\lambda_{\psi_2}), \quad c_{\psi_2} = \cos(\lambda_{\psi_2}), \quad s_{v2} = \sin(\lambda_{v2}), \quad c_{v2} = \cos(\lambda_{v2}),$$

$$sh_{v2} = \sinh(\lambda_{v2}), \quad ch_{v2} = \cosh(\lambda_{v2}),$$

the non-zero elements of the matrix $\mathbf{A}_I$ are

$$\mathbf{A}_{I_{1,1}} = s_{u1}, \quad \mathbf{A}_{I_{1,4}} = -LC_\theta,$$

$$\mathbf{A}_{I_{1,7}} = LS_\theta, \quad \mathbf{A}_{I_{1,9}} = LS_\theta,$$

$$\mathbf{A}_{I_{2,2}} = s_{w1} - sh_{w1}, \quad \mathbf{A}_{I_{2,3}} = c_{w1} - ch_{w1},$$

$$\mathbf{A}_{I_{2,4}} = -LS_\theta, \quad \mathbf{A}_{I_{2,7}} = -LC_\theta,$$

$$\mathbf{A}_{I_{2,9}} = -LC_\theta, \quad \mathbf{A}_{I_{3,2}} = \lambda_{w1}(c_{w1} - ch_{w1}),$$

$$\mathbf{A}_{I_{3,3}} = -\lambda_{w1}(s_{w1} + sh_{w1}), \quad \mathbf{A}_{I_{3,6}} = -\lambda_{w2},$$

$$\mathbf{A}_{I_{3,8}} = -\lambda_{w2}, \quad \mathbf{A}_{I_{4,1}} = -\lambda_{u1}c_{u1}C_\theta,$$

$$\mathbf{A}_{I_{4,2}} = -v_{w1}\lambda_{w1}^3 S_\theta(c_{w1} + ch_{w1}), \quad \mathbf{A}_{I_{4,3}} = v_{w1}\lambda_{w1}^3 S_\theta(s_{w1} - sh_{w1}),$$

$$\mathbf{A}_{I_{4,5}} = \sigma\lambda_{u2}, \quad \mathbf{A}_{I_{5,1}} = \lambda_{u1}c_{u1}S_\theta,$$

$$\mathbf{A}_{I_{5,2}} = -v_{w1}\lambda_{w1}^3 C_\theta(c_{w1} + ch_{w1}), \quad \mathbf{A}_{I_{5,3}} = v_{w1}\lambda_{w1}^3 C_\theta(s_{w1} - sh_{w1}),$$

$$\mathbf{A}_{I_{5,6}} = \sigma v_{w2}\lambda_{w2}^3, \quad \mathbf{A}_{I_{5,8}} = -\sigma v_{w2}\lambda_{w2}^3,$$

$$\mathbf{A}_{I_{6,2}} = -v_{w1}\lambda_{w1}^2(s_{w1} + sh_{w1}), \quad \mathbf{A}_{I_{6,3}} = -v_{w1}\lambda_{w1}^2(c_{w1} + ch_{w1}),$$

$$\mathbf{A}_{I_{6,7}} = L\sigma v_{w2}\lambda_{w2}^2, \quad \mathbf{A}_{I_{6,9}} = -L\sigma v_{w2}\lambda_{w2}^2,$$

$$\mathbf{A}_{I_{7,6}} = -\lambda_{w2}^2 s_{w2}, \quad \mathbf{A}_{I_{7,7}} = -\lambda_{w2}^2 c_{w2},$$

$$\mathbf{A}_{I_{7,8}} = \lambda_{w2}^2 sh_{w2}, \quad \mathbf{A}_{I_{7,9}} = \lambda_{w2}^2 ch_{w2},$$

$$\mathbf{A}_{I_{8,4}} = -\lambda_{u2}(\rho L s_{u2} + \lambda_{u2}M_t c_{u2}), \quad \mathbf{A}_{I_{8,5}} = \lambda_{u2}(\rho L c_{u2} - \lambda_{u2}M_t s_{u2}),$$

$$\mathbf{A}_{I_{9,6}} = -\lambda_{w2}^3(\rho L c_{w2} - \lambda_{w2}M_t s_{w2}), \quad \mathbf{A}_{I_{9,7}} = \lambda_{w2}^3(\rho L s_{w2} + \lambda_{w2}M_t c_{w2}),$$

$$\mathbf{A}_{I_{9,8}} = \lambda_{w2}^3(\rho L ch_{w2} + \lambda_{w2}M_t sh_{w2}), \quad \mathbf{A}_{I_{9,9}} = \lambda_{w2}^3(\rho L sh_{w2} + \lambda_{w2}M_t ch_{w2})$$

and the non-zero elements of the matrix $[\mathbf{A}_O]$ are

$$\mathbf{A}_{O_{1,1}} = s_{v1} - sh_{v1}, \quad \mathbf{A}_{O_{1,2}} = c_{v1} - ch_{v1},$$

$$\mathbf{A}_{O_{1,5}} = -L, \quad \mathbf{A}_{O_{1,7}} = -L,$$

$$\mathbf{A}_{O_{2,1}} = \lambda_{v1}(c_{v1} - ch_{v1}), \quad \mathbf{A}_{O_{2,2}} = -\lambda_{v1}(s_{v1} + sh_{v1}),$$

$$\mathbf{A}_{O_{2,4}} = -\lambda_{v2}C_\theta, \quad \mathbf{A}_{O_{2,6}} = -\lambda_{v2}C_\theta,$$

$$\mathbf{A}_{O_{2,8}} = -S_\theta, \quad \mathbf{A}_{O_{3,3}} = s_{\psi 1},$$

$$\mathbf{A}_{O_{3,4}} = \lambda_{v2}S_\theta, \quad \mathbf{A}_{O_{3,6}} = \lambda_{v2}S_\theta,$$

$$\mathbf{A}_{O_{3,8}} = -C_\theta, \quad \mathbf{A}_{O_{4,1}} = -v_1\lambda_{v1}^3(c_{v1} + ch_{v1}),$$

$$\mathbf{A}_{O_{4,2}} = v_1\lambda_{v1}^3(s_{v1} - sh_{v1}), \quad \mathbf{A}_{O_{4,4}} = \sigma v_2\lambda_{v2}^3,$$

$$\mathbf{A}_{O_{4,6}} = -\sigma v_2\lambda_{v2}^3, \quad \mathbf{A}_{O_{5,1}} = -L\chi_1\lambda_{v1}^2 S_\theta(s_{v1} + sh_{v1}),$$

$$\mathbf{A}_{O_{5,2}} = -L\chi_1\lambda_{v1}^2 S_\theta(c_{v1} + ch_{v1}), \quad \mathbf{A}_{O_{5,3}} = L\lambda_{\psi 1}c_{\psi 1}C_\theta,$$

$$\mathbf{A}_{O_{5,9}} = -\eta\lambda_{\psi_2}, \quad \mathbf{A}_{O_{6,1}} = -L\chi_1\lambda_{v1}^2 C_\theta(s_{v1} + sh_{v1}),$$

$$\mathbf{A}_{O_{6,2}} = -L\chi_1\lambda_{v1}^2 C_\theta(c_{v1} + ch_{v1}), \quad \mathbf{A}_{O_{6,3}} = -L\lambda_{\psi 1} c_{\psi 1} S_\theta,$$

$$\mathbf{A}_{O_{6,5}} = \eta\chi_2\lambda_{v2}^2, \quad \mathbf{A}_{O_{6,7}} = -\eta\chi_2\lambda_{v2}^2,$$

$$\mathbf{A}_{O_{7,4}} = -\lambda_{v2}^2 s_{v2}, \quad \mathbf{A}_{O_{7,5}} = -\lambda_{v2}^2 c_{v2},$$

$$\mathbf{A}_{O_{7,6}} = \lambda_{v2}^2 sh_{v2}, \quad \mathbf{A}_{O_{7,7}} = \lambda_{v2}^2 ch_{v2},$$

$$\mathbf{A}_{O_{8,8}} = -\lambda_{\psi 2} s_{\psi 2}, \quad \mathbf{A}_{O_{8,9}} = \lambda_{\psi 2} c_{\psi 2},$$

$$\mathbf{A}_{O_{9,4}} = -\lambda_{v2}^3(\rho L c_{v2} - M_t\lambda_{v2} s_{v2}), \quad \mathbf{A}_{O_{9,5}} = \lambda_{v2}^3(\rho L s_{v2} + M_t\lambda_{v2} c_{v2}),$$

$$\mathbf{A}_{O_{9,6}} = \lambda_{v2}^3(\rho L ch_{v2} + M_t\lambda_{v2} sh_{v2}), \quad \mathbf{A}_{O_{9,7}} = \lambda_{v2}^3(\rho L sh_{v2} + M_t\lambda_{v2} ch_{v2}).$$

Appendix B. Nomenclature

A_i	cross-sectional area of the ith beam
E_i	Young's modulus of the ith beam
G_i	shear modulus of the ith beam
$I_{yy}^{(i)}$	second moment of the area of the ith beam about yy-axis
$I_{zz}^{(i)}$	second moment of the area of the ith beam about zz-axis
J_i	area polar moment of inertia of the ith beam
L	ratio of the length of the second beam to the first beam
L_i	length of the ith beam
M_t	non-dimensional mass of the tip mass
T	system kinetic energy
U	system potential energy
$U_i(x_i)$	axial displacement eigenfunctions of the ith beam
$V_i(u_i)$	out-of-plane displacement eigenfunctions of the ith beam
$W_i(u_i)$	transverse displacement eigenfunctions of the ith beam
$\Psi_i(u_i)$	torsion eigenfunctions of the ith beam
m_t	mass of the tip mass
t	time
$u_i(x_i, t)$	axial displacement of the ith beam
$v_i(x_i, t)$	out-of-plane displacement of the ith beam
$w_i(x_i, t)$	transverse displacement of the ith beam
x_i	co-ordinate of the ith beam
$\psi_i(x_i, t)$	torsional angle of the ith beam
θ	orientation of the second beam relative to the first
η	ratio of the torsional stiffness of the second beam to the first beam
λ_{*i}	non-dimensional frequency of the ith beam with regard to $*$ variable

σ ratio of extensional force of the second beam to the first beam
χ_i ith beam ratio of the flexural stiffness to torsional stiffness
ξ_i non-dimensional co-ordinate of the ith beam
ρ ratio of the length density of the second beam to the first beam
ρ_i volume mass density of the ith beam
v slenderness ratio
ω natural frequency
$\dot{(\,)}$ time derivative
$(\,)'$ spatial derivative

References

[1] D.C.D. Oguamanam, G.R. Heppler, J.S. Hansen, Vibration of arbitrarily oriented two member open frames with tip mass, Journal of Sound and Vibration 209 (4) (1998) 651–669.
[2] A. Alexandropoulos, G. Michaltsos, K. Kounadis, The effect of longitudinal motion and other parameters on the bending eigenfrequencies of a simple frame, Journal of Sound and Vibration 106 (1) (1986) 153–159.
[3] K. Kounadis, K. Meskouris, The coupling effect of axial motion and joint mass on the lateral vibrations of a rigid jointed triangular frame, Earthquake Engineering and Structural Dynamics 15 (1987) 447–462.
[4] D. Sophianopoulos, K. Kounadis, The axial motion effect on the dynamic response of a laterally vibrating frame subjected to a moving load, Acta Mechanica 79 (1989) 277–294.
[5] C.H. Chang, P.Y. Wang, Y.W. Lin, Vibration of X-braced portal frames, Journal of Sound and Vibration 117 (2) (1987) 233–248.
[6] C.P. Filipich, B.H. Valerga de Greco, P.A.A. Laura, A note on the analysis of symmetric mode of vibrations of portal frames, Journal of Sound and Vibration 117 (1) (1987) 198–201.
[7] C.P. Filipich, P.A.A. Laura, In-plane vibrations of portal frames with end supports elastically restrained against rotation and translation, Journal of Sound and Vibration 117 (3) (1987) 467–474.
[8] P.A.A. Laura, B.H. Valerga de Greco, In-plane vibrations of frames carrying concentrated masses, Journal of Sound and Vibration 117 (3) (1987) 447–458.
[9] J.E. Mottershead, T.K. Tee, C.D. Foster, An experiment to identify the structural dynamics of a portal frame, Journal of Vibration and Acoustics 112 (1) (1990) 78–83.
[10] H.P. Lee, T.Y. Ng, In-plane vibration of planar frame structures, Journal of Sound and Vibration 172 (3) (1994) 420–427.
[11] A.S. Yigit, The effect of flexibility on the impact response of a two-link rigid-flexible manipulator, Journal of Sound and Vibration 177 (3) (1994) 349–361.
[12] J.L. Junkins, Y. Kim, Introduction to Dynamics and Control of Flexible Structures, AIAA, Washington, DC, 1993.
[13] H. Bang, Analytical solution for dynamic analysis of a flexible L-shaped structure, Journal of Guidance, Control and Dynamics 19 (1) (1996) 248–250.
[14] M. Gürgöze, Comment on 'Analytical solution for dynamic analysis of a flexible L-shaped structure', Journal of Guidance, Control and Dynamics 21 (2) (1998) 359.